Effects of target polarization and postcollision interaction on the electron-impact single ionization of Ne($2p$), Ar($3p$), and Na($3s$) atoms

G. Purohit,[1,2,*] Prithvi Singh,[1] Vinod Patidar,[1] Y. Azuma,[2] and K. K. Sud[1]

[1]*Department of Physics, School of Engineering, Sir Padampat Singhania University, Bhatewar, Udaipur-313 601, India*

[2]*Department of Materials and Life Sciences, Faculty of Science and Technology, Sophia University, 7-1, Kioi-cho, Chiyoda-ku, Tokyo 102-8554, Japan*

(Received 6 January 2012; revised manuscript received 22 January 2012; published 24 February 2012)

We report the perpendicular plane ionization results of (e, $2e$) triple-differential cross sections for the Ne($2p$) and Ar($3p$) atoms at the incident electron energies ranging from 5 to 50 eV above ionization potential for neon atoms and from 2 to 50 eV above ionization potential for the argon atoms. The present investigation has been done in the modified distorted wave Born approximation and it has been observed that postcollision interaction and polarization of target are important in the perpendicular plane ionization of atoms. We also present the results of triple-differential cross section for the doubly symmetric coplanar ionization of Na($3s$) atoms at the incident electron energy ranging from 6 to 60 eV above ionization potential. Thus we are able to see the effects of target polarization and postcollision interaction in coplanar as well as the perpendicular plane geometrical conditions. The results of our calculations for the Ne($2p$) and Ar($3p$) have been compared with the very recent measurements of Nixon *et al*. [K. L. Nixon, A. J. Murray, and C. Kaiser, J. Phys. B **43**, 085202 (2010)] and the results of coplanar ionization of Na($3s$) have been compared with the experimental data of Murray [A. J. Murray, Phys. Rev. A **72**, 062711 (2005)]. It is observed that there are certain discrepancies between theoretical and experimental results which indicate that further theoretical efforts are required to understand the cross section trends of neon, argon, and sodium atoms. The cross section in the perpendicular plane ionization exhibits complex variations as a function of incident energy and target.

DOI: 10.1103/PhysRevA.85.022714 PACS number(s): 34.80.Dp, 34.80.Bm

I. INTRODUCTION

The ionization of atoms and molecules by charged particle impact is one of the fundamental and most interesting process in atomic physics. In the last few decades there has been a considerable amount of progress in the theoretical description of the electron-impact ionization processes. The kinematically complete studies of electron-impact single ionization, called (e, $2e$) processes, were initiated nearly 40 years ago [1,2] and since then it has been used to probe the structure of the ionized target or to understand the dynamics of (e, $2e$) reactions [3]. A wide range of data are available for the ionization of hydrogen and helium atoms, even for more complex atomic and molecular targets [4], surfaces [5], and clusters [6]. Besides the direct knockout of the electron (i.e., direct ionization) different complex processes such as double ionization [7], simultaneous excitation ionization [8], and autoionization [9] have also been investigated. The (e, $2e$) on the hydrogen atom may now be considered to be a solved problem [10,11] and significant understanding of the ionization of two-electron systems such as helium and heliumlike targets has been developed [12]. The theoretical methods such as exterior complex scaling (ECS) [10] and convergent close coupling (CCC) [11] have obtained the exact solution of the electron-hydrogen atom scattering problem. These nonperturbative theories are in the process of development for more complex systems such as lithium atoms and hydrogen molecules [13,14]. For even more complex many-electron systems, such as heavier noble gas targets, alkali, and alkali earth metals, the most successful alternative is the distorted wave Born approximation (DWBA). The DWBA has produced reasonable agreement of triple-differential cross section (TDCS) with experimental data at incident electron energies 200 eV and above [15]. At lower incident electron energies different physical processes such as Coulomb repulsion between scattered and ejected electrons in the final state [often referred to as postcollisional interaction (PCI)], electron exchange, target polarization, etc., need to be considered. It has been found that inclusion of these effects in the standard DWBA formalism improves the description of the (e, $2e$) process quiet well (see [16–20] and references cited therein). Apart from this, the perturbation approaches provide insight into the collision dynamics because there remains a possibility of switching on or off a particular interaction and of seeing the effect on the resultant TDCS. However, still there are many discrepancies between the theoretical results and experimental data at the low and intermediate incident electron energies.

Most of the (e, $2e$) measurements and theoretical studies have been performed in coplanar geometry where both the final-state electrons move in the same plane as the incident electron. In the coplanar scattering the cross section is observed with the well known binary and recoil peaks due to the first-order projectile target interaction. The coplanar studies show that there is a maximum probability for ejecting the target electron in the direction of momentum transfer from the projectile to the target and there is a smaller probability for the ejection of electron in the opposite direction of momentum transfer. These processes are responsible for production of binary and recoil peaks respectively. In recent years there has been investigation of (e, $2e$) processes which concentrated on

*g_vpurohit@yahoo.com; ghanshyam.purohit@spsu.ac.in

the non-coplanar geometries. The systematic investigation of these geometrical arrangements was initiated following the measurements done by Murray and group [21,22] and the higher-order or multiple scattering processes were identified by these investigations. Schulz *et al.* [23] obtained the first three-dimensional cross section images for ion-impact ionization in the out-of-plane geometry and it was observed that the projectile scattering due to the Coulomb potential of the nucleus in addition to the binary collision is responsible for the trends of TDCS in the perpendicular plane [24]. Al-Hagan *et al.* [25] reported the perpendicular plane ionization of the helium atom and the hydrogen molecule and discussed the salient features of the perpendicular plane ionization. Ren *et al.* [26] reported a detailed experimental and theoretical study of low-energy electron-impact ionization for H_2 and He targets. Both of the above mentioned studies [25,26] showed that the nonperturbative calculations are in good agreement with the He atom results and there are some discrepancies for the hydrogen molecule in the recoil peak region. Very recently Nixon *et al.* [27] reported the low-energy $(e, 2e)$ studies of the noble gas targets in the perpendicular plane geometry. They carried out the $(e, 2e)$ measurements from near-threshold to the intermediate energy range where the outgoing electrons carry equal energies. The particular geometrical arrangement (perpendicular plane) and the energy range provide a stringent test of the theoretical models dealing with the scattering problem. It is necessary to consider the effects such as multiple collisions, target polarization, distortions of the wave functions, and postcollisional interaction to understand the collision dynamics of low-energy perpendicular plane ionization. The theoretical models such as distorted wave Born approximation (DWBA), convergent close coupling (CCC), and time dependent close coupling (TDCC) have been successful for describing the ionization from the simpler targets such as atomic H and He.

We present in this paper the results of our modified distorted wave Born approximation calculation for the electron-impact single ionization of Ne and Ar atoms in perpendicular plane geometry. To our knowledge there is no other theoretical study available for the perpendicular plane ionization of Ne and Ar targets following the measurements of Nixon *et al.* [27], so our present attempt will be very useful in understanding the collision dynamics of perpendicular plane ionization of the heavier noble gas targets Ne and Ar. We include target polarization effect and postcollision interaction (PCI) in our standard DWBA calculation and discuss the role of postcollision interaction and target polarization in perpendicular plane geometry for the ionization of Ne and Ar atoms. We compare the results of our calculations with the recent measurements of Nixon *et al.* [27]. For a comparison between perpendicular plane ionization and coplanar ionization of atoms in similar kinematic conditions and also to see the effect of target polarization and PCI in both geometrical conditions, we also report the results of our calculation of TDCS for the coplanar symmetric ionization of Na($3s$) atoms. We have selected Na($3s$) for present study since the coplanar ionization of sodium ($3s$) atoms has been of recent interest for those working in the field [28–32] following the experimental measurements of Murray [20]. All of the above mentioned theoretical calculations [28–32] could give a reasonably good agreement with the experimental results but with certain discrepancies. We compare our results with the experimental data of Murray [33] and discuss the trends of TDCS in comparison to the perpendicular plane ionization of Ne and Ar atoms. We present the theoretical model of our present calculations in next section.

II. THEORY

The electron-impact single ionization [i.e., $(e, 2e)$] process on a target A is expressed as

$$e^- + A \rightarrow A^+ + e^- + e^-. \tag{1}$$

The triple-differential cross section for the $(e, 2e)$ process on an atom as in Eq. (1) may be written as

$$\frac{d^3\sigma}{d\Omega_1 d\Omega_2 dE_1} = (2\pi)^4 \frac{k_1 k_2}{k_0} \sum_{av} |T(k_1,k_2,k_0)|^2, \tag{2}$$

with

$$T(k_1,k_2,k_0) = \langle k_1 k_2 | T | \psi_{nl} k_0 \rangle.$$

The expression in Eq. (2) includes a sum over final and average over initial magnetic and spin-state degeneracy. The T matrix in Eq. (2) is the reaction amplitude; it couples the initial states ψ_{nl} and the final states. T includes interaction between the incident and target electrons and the nucleus. It is the part of the TDCS that is the subject of approximation. The T-matrix element, which represents the ionization amplitude, is conveniently written in terms of distorted waves as

$$\langle k_1 k_2 | T | \psi_{nl} k_o \rangle = \langle X_1^{(-)}(k_1) X_2^{(-)}(k_2) | v_3 | \psi_{nl} X_0^{(+)}(k_0) \rangle. \tag{3}$$

E_0, E_1, E_2 and $\mathbf{k_0}, \mathbf{k_1}, \mathbf{k_2}$ are energies and momenta of incident, scattered, and ejected electrons, respectively. The electron-electron potential v_3 is responsible for ionization. The initial state ψ_{nl} contains an electron bound to the atom core with separation energy E_b. The initial-state distorted waves $X^{(+)}$ are generated in the initial-state distorting potential U_i. The initial-state distorting potential consists of the nuclear contribution plus a spherically symmetric approximation for the interaction between the projectile electron and the target electrons. The final-state distorted waves $X^{(-)}$ are obtained in the final-state distorting potential which consists of the nuclear contribution plus a spherically symmetric approximation for the interaction between the continuum electron and the electrons in the ion.

Equation (2) in terms of direct and exchange amplitudes may be written as

$$\frac{d^3\sigma}{d\Omega_1 d\Omega_2 dE_1} = (2\pi)^4 \frac{k_1 k_2}{k_0} \sum_{av} [|f|^2 + |g|^2 - \mathrm{Re}(f^* g)], \tag{4}$$

where

$$f = \langle X_1^{(-)}(k_1,r_1) X_2^{(-)}(k_2,r_2) | v_3 | X_0^{(+)}(k_0,r_1) \psi_{nl}(r_2) \rangle, \tag{5}$$

$$g = \langle X_1^{(-)}(k_1,r_2) X_2^{(-)}(k_2,r_1) | v_3 | X_0^{(+)}(k_0,r_1) \psi_{nl}(r_2) \rangle. \tag{6}$$

In the present investigation both the outgoing electrons share equal energies and are emitted at the same angle with reference to the incident electron, so the direct and exchange

amplitudes are equal; i.e., $f = g$; here $v_3 = \frac{1}{|r_1 - r_2|}$ is the interaction potential between the incident and target electrons responsible for the ionization, $X_0^{(+)}$ is the distorted wave function for the incident electron; $X_1^{(-)}$ and $X_2^{(-)}$ represent the distorted wave functions for the two outgoing electrons and each is orthogonalized with respect to ψ_{nl}. Equations (5) and (6) are direct and exchange amplitudes for ionization from the (n, l) shell of the target atom where ψ_{nl} is the corresponding target orbital from which the ionization is taking place, and n and l are the principal and orbital quantum numbers, respectively. We have used Hartree-Fock orbitals of Clementi and Roetti [34] for ψ_{nl}. As mentioned above the distorted wave function for the incident electron is generated in the equivalent local ground-state potential of the atom whereas the distorted wave functions for the outgoing electrons are generated in the equivalent local ground-state potential of the ion. For the work reported here we have made a careful check to ensure that the cross sections converge satisfactorily. The spin-averaged static-exchange potential of Furness and McCarthy [35] as modified by Riley and Truhlar [36] has been used; it is given as

$$V_E(r) = 0.5(E_0 - V_D(r) - \{[E_0 - V_D(r)]^2 + 4\pi\rho(r)\}^{1/2}), \tag{7}$$

where $\rho(r)$ is the electron density. The direct distorting potential $V_D(r)$ for the incident electron is obtained from the target radial orbital $u_{nl}(r)$ [37] as

$$V_D(r) = -\frac{Z}{r} + \sum_{nl} N_{nl} \int dr'[u_{nl}(r')]^2/r_>, \tag{8}$$

where $r_>$ is the greater of r and r'. The details about the integration of the radial matrix element are described by McCarthy [37] and not reproduced here for brevity. The equivalent local ground-state potential U_i, which is the distorting potential, is the sum of exchange and direct potentials and is expressed as follows:

$$U_i = V_D(r) + V_E(r), \tag{9}$$

$$U_i = V_D(r) + 0.5(E_0 - V_D(r) - \{[E_0 - V_D(r)]^2 + 4\pi\rho(r)\}^{1/2}). \tag{10}$$

We have modified the distorting potential [Eq. (10)] used to calculate distorted waves $X_0^{(+)}$, $X_1^{(-)}$, and $X_2^{(-)}$, adding the correlation-polarization potential V_{CP} to observe the effect of electron correlation and target polarization on the trend of TDCS. The fundamental form of the short-range correlation plus long-range polarization potential may be approximated by means of local density functional theory (Padial and Norcross [38]; Perdew and Zunger [39]; Yuan and Zhang [40]) as follows:

$$\begin{aligned} V_{CP}(r) &= V_{SR}^{\text{Corr}}(r), \quad r \leqslant r_0, \\ &= -\frac{\alpha_d}{2r^4}, \quad r > r_0, \end{aligned} \tag{11}$$

where α_d is dipole polarizability of the target and we have used short-range correlation potential similar to [38]. The point r_0 is the intersection of the short-range correlation and long-range polarization potential and roughly it may be taken as the radius of atomic orbital.

We have included PCI in our DWBA calculations using the Ward-Macek factor (M_{ee}) [41]. The M_{ee} is defined as

$$M_{ee} = N_{ee}|_1F_1(-i\lambda_3, 1, -2k_3 r_{3\text{ave}})|^2,$$

where

$$N_{ee} = \frac{\gamma}{e^\gamma - 1}, \quad \gamma = -\frac{2\pi}{|k_1 - k_2|},$$
$$\lambda_3 = -\frac{1}{|k_1 - k_2|},$$

and

$$r_{3\text{ave}} = \frac{\pi^2}{16\varepsilon}\left(1 + \frac{0.627}{\varepsilon}\sqrt{\varepsilon}\ln\varepsilon\right)^2,$$

where ε is the total energy of the two exiting electrons.

The TDCS incorporating PCI through M_{ee} is now written as

$$\frac{d^3\sigma}{d\Omega_1 d\Omega_2 dE_1} = M_{ee}(2\pi)^4 \frac{k_1 k_2}{k_0} \sum_{av} [|f|^2 + |g|^2 - \text{Re}(f^* g)]. \tag{12}$$

III. RESULTS AND DISCUSSION

The results of $(e, 2e)$ TDCS for the perpendicular plane ionization of Ne$(2p)$ and Ar$(3p)$ are presented in Figs. 1–3. The present calculations have been done in modified distorted wave Born approximation for the ionization of Ne$(2p)$ at incident electron energies from 5 to 50 eV above ionization potential (IP) and for the ionization of Ar$(3p)$ at incident electron energies from 2 to 50 eV above IP. In each case the outgoing electrons share equal energies. The dashed curve represents the DWBA calculations including postcollision interaction (PCI) and the solid curve represents the DWBA calculations including correlation-polarization potential and PCI. These results are presented in the atomic unit (a.u.) scale. We compare the results of our calculations with the recent measurements of Nixon *et al.* [27]. The perpendicular plane ionization of targets include multiple scattering effects where the incident electron interacts with the target nucleus as well as the bound electrons. In the present investigation both the outgoing electrons share equal energies and ionization is taking place for the incident electron energies ranging from near the ionization potential to 50 eV above IP. Thus the perpendicular plane ionization provides a stringent test of the theoretical models. Our present attempt is useful in understanding the collision dynamics of Ne and Ar, since following the measurements of Nixon *et al.* [27] no other theoretical study is available to compare. The results for the ionization of Ne$(2p)$ are presented in Fig. 1. At the lowest incident electron energy (5 eV above IP) for the ionization of neon target two side lobes and a local minimum (at mutual angle $\phi = 180^\circ$) are observed in our calculations [Fig. 1(a)]. However, the experimental data have a broad peak at $\phi = 180^\circ$, similar to the case of ionization of He. The minimum at $\phi = 180^\circ$ may be due to the momentum distribution of the p electron as ionization is taking place from the p orbital of Ne$(2p)$. The reason for the side lobes may be ascertained as the elastic scattering of the incident electron from the

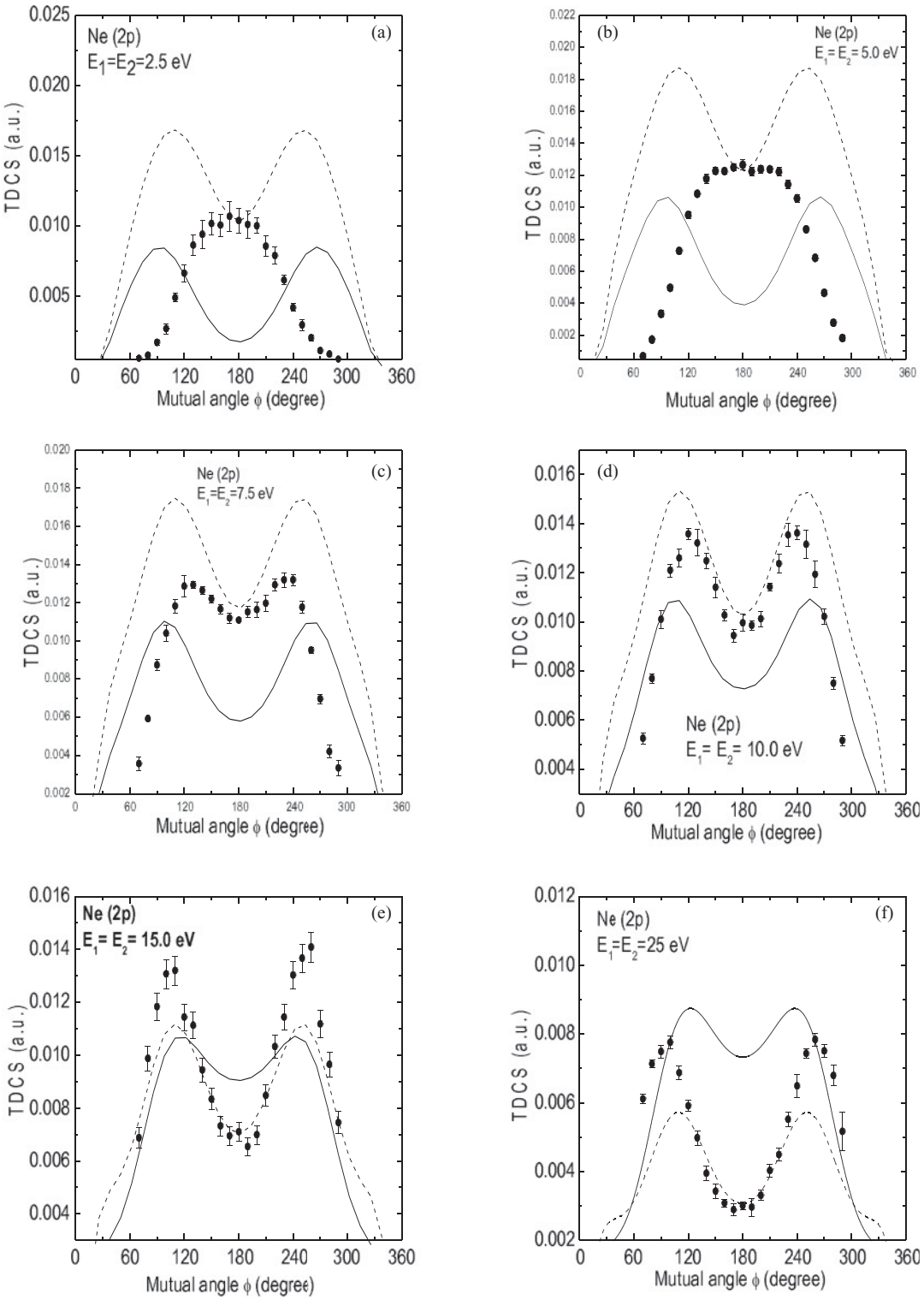

FIG. 1. Triple-differential cross section of Ne($2p$) atoms as a function of the mutual angle between the two outgoing electrons in the perpendicular plane geometry. Dashed curve: present DWBA calculation with PCI; solid curve: present DWBA calculation including correlation-polarization potential and PCI. Filled circles: Experimental data of Nixon *et al*. [27]. The experimental data are normalized to the dashed curve for best visual fit. The theoretical results are in the atomic unit (a.u.) scale. Kinematics is displayed in each frame.

core. However, as observed in the helium case these side lobes should be observed at the mutual angles $\phi = 90^\circ$ and $\phi = 270^\circ$. Our present DWBA calculations including PCI (dashed curve) produce the side lobes at different angles but the DWBA calculations with target polarization and PCI provide the side peaks nearly at the mutual angles $\phi = 90^\circ$ and $\phi = 270^\circ$. This observation suggests that along with the PCI the target polarization is a very important effect (as also

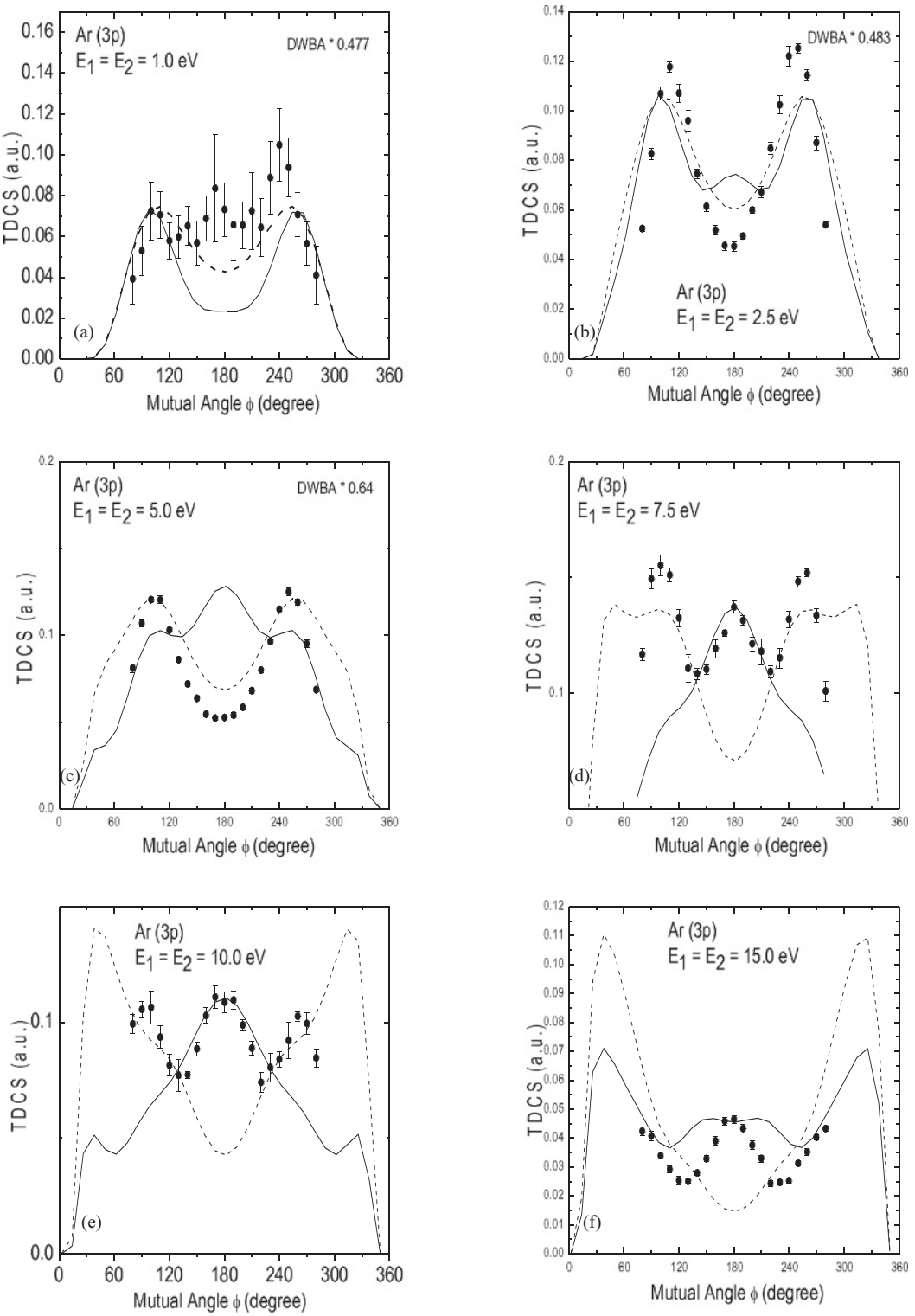

FIG. 2. Same as Fig. 1 but for the Ar($3p$) atoms. For better comparison some of the DWBA results (dashed curve) have been multiplied by the factor shown in respective frames.

indicated by Nixon *et al*. [27]) which should be considered properly for the perpendicular plane ionization of atomic targets. As expected the zero cross sections are observed for the electrons emerging at the same angles $\phi = 0^\circ$ and $\phi = 360^\circ$ due to the postcollisional interactions. The experimental data have a wider peak centered around the mutual angle $\phi = 180^\circ$ at incident electron energy 10 eV IP for Ne($2p$). However, our calculations continue to show a similar trend with a minimum at $\phi = 180^\circ$ and two side lobes. At the other incident electron energies from 15 eV above IP to 50 eV above IP the experimental data also exhibit a trend of TDCS with a minimum at $\phi = 180^\circ$ and two side lobes. The side lobes

shift away from the central minimum as the incident electron energy increases and the depth of minimum also increases [see Figs. 1(c)–1(f)]. As predicted by Nixon *et al*. [27] the mechanism of perpendicular plane ionization of Ne($2p$) seems to be different from that of the ionization of He ($1s$) atom in similar geometrical arrangements. However, the role of PCI is, as expected, at the lowest incident energies. The mechanism of perpendicular ionization of the He atom may be considered as well understood [25,26] but more theoretical efforts are required to understand the trend of TDCS for the case of neon atoms.

We report the results of our (e, $2e$) TDCS for the ionization of Ar($3p$) at all nine incident electron energies ranging from 2 to 50 eV ionization potential, the same as the measurements of Nixon *et al*. [27]. At the incident electron energy which is just 2 eV above ionization potential, both of our calculations with PCI as well as polarization potential and PCI provide a two-peak structure with a minimum at the mutual angle $\phi = 180^\circ$ [Fig. 2(a)]. The experimental trends are not very clear at this energy and both of our calculations produce good agreement with the side lobes after inclusion of PCI, so it is clear that PCI is very important at this energy, as expected by the Wannier model [42]. When the incident electron energy is increased to 5 eV above IP the DWBA calculation with PCI provides a very good agreement with the experimental data with the same position of side lobes and a minimum at the mutual angle $\phi = 180^\circ$ [dashed curve in Fig. 2(a)]. However, the inclusion of polarization potential produces a peak at the position $\phi = 180^\circ$ with the two side lobes similar to the measurements and DWBA with PCI calculations. As incident electron energy is further increased the experimental trends also show a peak at the central position $\phi = 180^\circ$ with two side lobes; this central peak initially increases up to the incident electron energy 30 eV above IP and then again decreases and a minimum is observed at the $\phi = 180^\circ$ for the incident electron energy 50 eV above IP. The DWBA calculations with PCI (dashed curves) give a reasonable agreement with the experimental data up to incident electron energy 10 eV above IP [see Figs. 2(a)–2(c)] but the central peak which is present in experimental data after this energy is not observed. The DWBA calculations with PCI give nearly good agreement in the side lobe region for all the incident electron energies up to 50 eV above IP, but the side lobes are shifted more away from the mutual angle $\phi = 180^\circ$; however, the side lobes are also shifted in the experimental data as the incident electron energy is increased. The DWBA calculations with polarization potential and PCI are able to exhibit the central peak as observed in the experimental data for the incident electron energies 15 and 20 eV above IP [Figs. 2(d) and 2(e)] but the two side lobes are reduced very much in comparison to the central peak magnitude. For the further high incident electron energies [Figs. 3(a) and 3(b)], the calculation with polarization potential shows a slight minimum instead of a small peak in the experimental data. Both of our calculations again provide a reasonable agreement with the experimental data for the incident electron energy 50 eV above IP [Fig. 3(c)]. Thus the present DWBA calculations with PCI provide a two-lobe structure with the minimum at $\phi = 180^\circ$, with some change in the trends of TDCS and positions of the peak, which is nearly the same behavior as observed for similar calculations for the perpendicular plane ionization of Ne. However, the DWBA calculations with PCI and polarization potential produce a central peak for some of the incident electron energies and again produce a minimum for the highest incident electron energy used in the present investigation. Since the static polarization of the argon atom is nearly eight times higher

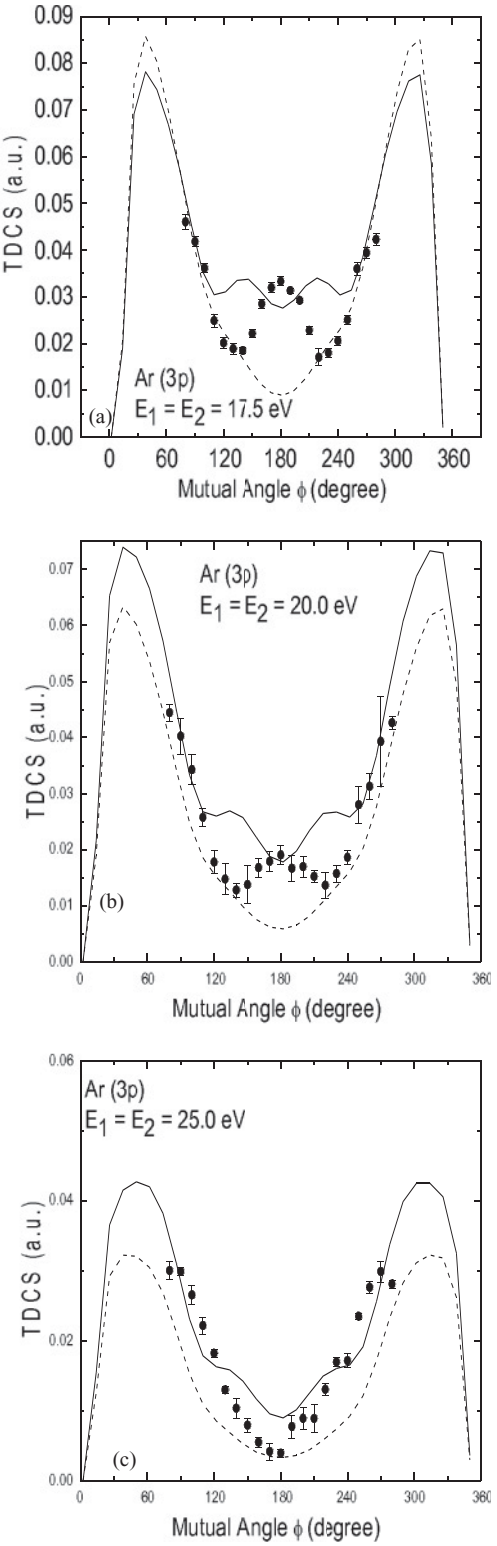

FIG. 3. Same as Fig. 1 but for Ar($3p$) atoms.

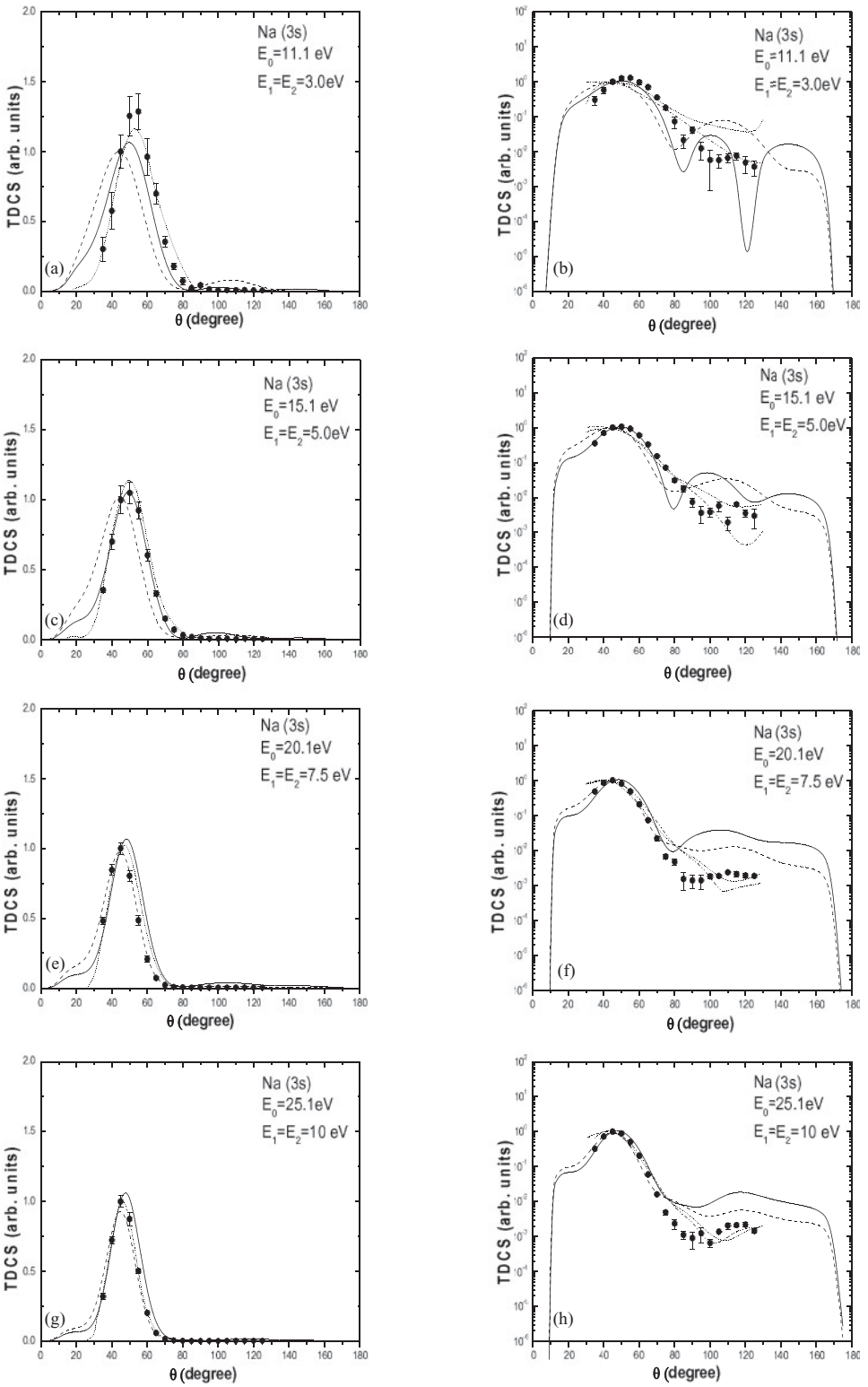

FIG. 4. Triple-differential cross section of Na(3s) atoms as a function of symmetric angle $\theta_1 = -\theta_2 = \theta$ in the coplanar symmetric geometry; filled circles: experimental data of Murray [33]; dashed curve: present DWBA calculation including PCI; solid curve: present DWBA calculation including correlation-polarization potential and PCI. Dotted curve (linear scale): Calculations of Bray *et al*. [33]. Dash-dotted and dotted curves (semilogarithmic scale) are the DWBA calculations of Srivastava *et al*. [28] in the R model and JMS models, respectively. The experimental data [33] and other theoretical results have been normalized to unity at the symmetric scattering angle $\theta = 45^\circ$. Kinematics is displayed in each frame.

than the neon atom, as also pointed out by Nixon *et al*. [27], we confirm that the polarization potential has a significant role to play in the collision dynamics of perpendicular plane ionization.

The results of the $(e, 2e)$ triple-differential cross sections for the coplanar ionization of Na(3s) are presented in Figs. 4 and 5. The calculations have been performed in coplanar geometry in the conditions of equal energy sharing between the two outgoing electrons. The incident electron energies used in the present investigation are 11.1, 15.1, 20.1, 25.1, 35.1, 45.1, 55.1, and 65.1 eV, which means the equal energy shared by the each electron is 3, 5, 7.5, 10, 15, 20, 25, and 30 eV. Having one valence electron in the outermost shell, the Na(3s) has been of particular interest for workers in the field and particularly, the coplanar doubly symmetric ionization case has been explored very well by the experimental [33] as well as by

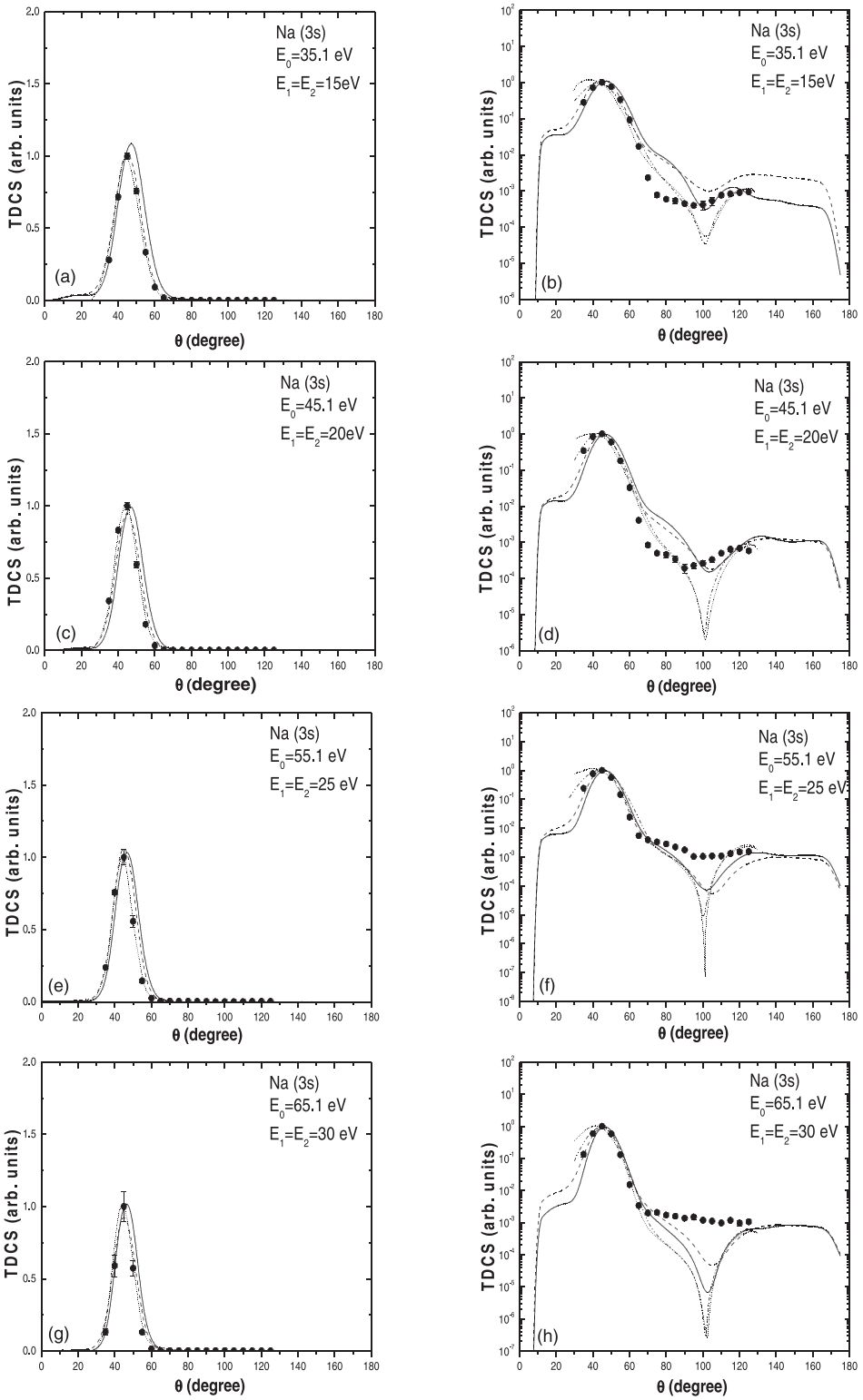

FIG. 5. Same as Fig. 4.

the theoretical workers [28–32]. The dashed curve represents the standard DWBA results and the solid curve represents the DWBA calculations including the correlation-polarization potential. We compare our modified DWBA results with the theoretical results of Bray *et al*. [30] and Srivastava *et al*. [28] and the experimental data of Murray [33]. All the theoretical and experimental results have been normalized to unity at the symmetric scattering angle $\theta = 45^\circ$ for a better comparison. We have presented the results of $(e, 2e)$ TCDS on a linear as well as a semilogarithmic scale; the finer structures present in the TDCS are visible only in the semilogarithmic scale plot. The solid curve represents our modified DWBA results which include correlation-polarization potential and postcollision interaction using M_{ee}; the dashed curve represents our DWBA calculations including postcollision interaction only. The dotted curve (linear scale) represents the CCC calculations of Bray

et al. [30]. In the semilogarithmic curve the dash-dotted and dotted curves are the DWBA calculations of Srivastava *et al*. [28] in which PCI has been included through angle-dependent effective charges using the R model and the JMS model, respectively. The R model has been proposed by Rudge [43] for e-H scattering and the JMS model has been suggested by Jones *et al*. [44]. The solid circles are experimental data of Murray [33]. To date there are few attempts [28–32], as mentioned in the Introduction of this paper, to explain the features of TDCS of doubly symmetric $(e, 2e)$ processes on Na($3s$) target. All of these calculations done in the different theoretical formalisms have a mixed degree of agreement with the experimental results. Hitawala *et al*. [29] have calculated TDCS using spin-averaged static-exchange potential [34] and included target polarization in the standard DWBA formalism. Li *et al*. [32] have reported the results of TDCS using modified semiclassical exchange potential [45] and also included PCI in the standard DWBA formalism. However, Srivastava *et al*. [28] have included PCI in the standard DWBA formalism through effective charges. Bray *et al*. [30] and Jia and Sun [31] have reported the results of their calculations for the doubly symmetric ionization of sodium atom in the CCC and DS3C (dynamically screened 3-Coulomb) formalism, respectively. However, they have presented their results on the linear scale. In the present attempt, we report the results of TDCS for the coplanar doubly symmetric $(e, 2e)$ processes on Na($3s$) target in modified DWBA formalism. We have modified DWBA by including correlation-polarization potential (which is a function of electron density—a better choice to include polarization potential at low energies) and PCI (through Ward-Macek factor M_{ee}). We critically analyze our results and other available theoretical results so that a new direction can be obtained to understand the collision dynamics of the sodium atom in the coplanar symmetric geometry.

The main features of the TDCS observed in all the above mentioned studies may be summarized as follows. In the coplanar doubly symmetric ionization of Na($3s$) a forward peak is observed near $\theta = 45^\circ$ due to the single-scattering mechanism or direct collision between the projectile electron and the target electron. A backward-scattering peak is observed near $\theta = 135^\circ$, which may be due to the double-scattering process in which the projectile first elastically scatters off the nucleus and then has a free collision with the bound electron (as predicted for the case of Ca atom [46]). The inclusion of postcollisional interaction (PCI) by the Ward and Macek factor makes the zero cross section for the forward ($\theta = 0^\circ$) and backward ($\theta = 180^\circ$) emission. Apart from the forward- and backwardscattering peaks few dips are observed in the TDCS profiles (which are only visible in the semilogarithmic plot of the TDCS versus symmetric-scattering angle profile). These dips may be present in the TDCS profile due to interference between the incoming and outgoing wave functions as explained earlier for the coplanar ionization from the Ca atoms [17]. At the incident electron energy 11.1 eV the results of Bray *et al*. [30] [short dotted curve in Fig. 4(a)] and Jia and Sun [31] (not shown in this paper) have very good agreement with the experimental results and we observe that our DWBA calculations including polarization potential and PCI are also able to produce the nearly correct trend of TDCS at this incident energy. As incident electron energy is increased from 11.1 to 65.1 eV the results of our present calculations as well as the results of Bray *et al*. [30] and Jia and Sun [31] are in very good agreement with the experimental results plotted on the linear scale; however, the TDCS results plotted on the semilogarithmic scale show discrepancies with the experimental data in the backward-scattering region. Our calculations including target polarization and PCI are able to produce most of the trends of TDCS in the forward-scattering region and have very good agreement with the experimental results, but as we can observe none of the calculations are able to produce the trends of TDCS as observed in the experimental results of Murray [33] for the backward-scattering angles.

IV. CONCLUSIONS

We have presented the results of our calculations for the perpendicular plane ionization of Ne($2p$) and Ar($3p$) atoms at all the incident electron energies used in the measurements of Nixon *et al*. [27]. We observe that the DWBA calculation with inclusion of PCI and polarization potential is able to give a mixed degree of agreement with the experimental data. The PCI is found to be important at the lower incident electron energies for both the targets investigated and polarization potential also plays an important role in case of the perpendicular plane ionization in the incident electron energy range of the present investigation; it seems to be more important for the targets of higher polarizability. The agreement with the measurements [27] is found to be good for the Ne($2p$) target in the intermediate energies and for the Ar($3p$) target at the low and high energies used in the present investigation. Thus, there are still many discrepancies in the agreement with the experimental results which is due to the complex processes involved in the perpendicular plane ionization of many electron targets, including neon and argon. The perpendicular plane ionization of He atoms has been well explained by the theoretical models such as DWBA, CCC, and TDCC (see [25,26] and references cited therein) but we feel that the proper explanation of the ionization of neon and argon atoms requires more theoretical efforts and our present attempt may be useful in this direction. We have also presented our results of $(e, 2e)$ TDCS for incident electron energies 11.1, 15.1, 20.1, 25.1, 35.1, 45.1, 55.1, and 65.1 eV (from excess energy 6–60 eV) for the coplanar doubly symmetric ionization of the sodium target. We observe that our modified DWBA results (which include correlation-polarization potential and PCI) are able to produce most of the trends of TDCS in the coplanar double symmetric geometry as observed in the experimental data [33] but still there exist a few discrepancies at very low incident electron energies. The polarization effect plays an important role at the incident electron energies used in the present investigation in the coplanar symmetric geometry; however, the effect of PCI is only significant for a few lower incident electron energies. All the previously available calculations [28–32] have a reasonable amount of agreement with the experimental data but the present attempt further improves the agreement between theory and measurements. Finally, we conclude that further studies with the proper treatment of polarization, exchange, electron correlation, and higher-order effects are required to improve the understanding

of collision dynamics of Ne($2p$) and Ar($3p$) atoms in the perpendicular plane and Na($3s$) in the coplanar symmetric geometry.

ACKNOWLEDGMENTS

We are thankful to the referee for providing constructive suggestions for the improvement of the presentation of the manuscript. We thank Professor Andrew James Murray for providing experimental data. G.P. would like to thank Professor Jim Babb and Professor Hossein Sadeghpour for useful discussions during his stay at the Institute of Theoretical Atomic, Molecular and Optical Physics (ITAMP), Harvard-Smithsonian Center for Astrophysics, Cambridge, USA. G.P. would also like to thank Privatdozent Dr. Alexander Dorn and Dr. Bennaceur Najjari for useful discussions during his stay at Max-Planck-Institut für Kernphysik, Heidelberg, Germany. P.S. acknowledges financial support in the form of a scholarship provided by Sir Padampat Singhania University (SPSU) for the research work; V.P. acknowledges the Science and Engineering Research Council (SERC), Department of Science Technology (DST), Government of India, for the Fast Track Young Scientist Research Grant (Grant No. SR/FTP/PS-17/2009).

[1] H. Ehrhardt, M. Schulz, M. Tekaat, and K. Willmann, Phys. Rev. Lett. **22**, 89 (1969).
[2] U. Amaldi, A. Egidi, R. Marconero, and G. Pizzella, Rev. Sci. Instrum. **40**, 1001 (1969).
[3] A. Lahmam-Bennani, J. Electron Spectrosc. Relat. Phenom. **123**, 365 (2002).
[4] M. Takahashi, N. Watanabe, Y. Khajuria, Y. Udagawa, and J. H. D. Eland, Phys. Rev. Lett. **94**, 213202 (2005).
[5] S. Samarin, O. M. Artamonov, A. D. Sergeant, J. Krischner, A. Morozov, and J. F. Williams, Phys. Rev. B **70**, 073403 (2004).
[6] M. Vos, S. A. Canney, I. E. McCarthy, S. Utteridge, M. T. Michalewicz, and E. Weigold, Phys. Rev. B **56**, 1309 (1997).
[7] C. Jia, A. Lahmam-Bennani, A. Duguet, L. Avaldi, M. Lecas, and C. Dal Capello, J. Phys. B **35**, 1103 (2002).
[8] S. Bellm, J. Lower, K. Bartschat, X. Guan, D. Weflen, M. Foster, A. L. Harris, and D. H. Madison, Phys. Rev. A **75**, 042704 (2007).
[9] J. Lower and E. Weigold, J. Phys. B **23**, 2819 (1990).
[10] T. N. Rescigno, M. Baertschy, W. A. Isaacs, and C. W. McCurdy, Science **286**, 2474 (1999).
[11] I. Bray, Phys. Rev. Lett. **89**, 273201 (2002).
[12] I. Bray, D. V. Fursa, A. S. Kheifets, and A. T. Stelbovics, J. Phys. B **35**, R117 (2002).
[13] A. S. Kheifets, D. V. Fursa, C. W. Hines, I. Bray, J. Colgan, and M. S. Pindzola, Phys. Rev. A **81**, 023418 (2010).
[14] J. Colgan, M. S. Pindzola, F. Robicheaux, C. Kaiser, A. J. Murray, and D. H. Madison, Phys. Rev. Lett. **101**, 233201 (2008).
[15] S. Jones, D. H. Madison, and M. Baertschy, Phys. Rev. A **67**, 012703 (2003).
[16] G. Purohit, Vinod Patidar, and K. K. Sud, Phys. Lett. A **374**, 2654 (2010).
[17] G. Purohit, Vinod Patidar, and K. K. Sud, Phys. Scr. **80**, 065301 (2009).
[18] G. Purohit, Vinod Patidar, and K. K. Sud, J. Electron Spectrosc. Relat. Phenom. **175**, 1 (2009).
[19] G. Purohit, V. Patidar, and K. K. Sud, J. Phys: Conf. Ser. **288**, 012008 (2011).
[20] G. Purohit, V. Patidar, and K. K. Sud, J. Phys: Conf. Ser. **235**, 012013 (2010).
[21] A. J. Murray, M. B. J. Woolf, and F. H. Read, J. Phys. B **25**, 3021 (1992).
[22] A. J. Murray and F. H. Read, Phys. Rev. A **47**, 3724 (1993).
[23] M. Schulz, M. Moshammer, D. Fischer, H. Kollmus, D. H. Madison, S. Jones, and J. Ullrich, Nature (London) **422**, 48 (2003).
[24] M. Schulz, M. Durr, B. Najjari, R. Moshammer, and J. Ullrich, Phys. Rev. A **76**, 032712 (2007).
[25] O. Al-Hagan, C. Kaiser, A. J. Murray, and D. H. Madison, Nat. Phys. **5**, 59 (2009).
[26] X. Ren, A. Senftleben, T. Pfluger, A. Dorn, J. Colgan, M. S. Pindzola, O. Al-Hagan, D. H. Madison, I. Bray, D. V. Fursa, and J. Ullrich, Phys. Rev. A **82**, 032712 (2010).
[27] K. L. Nixon, A. J. Murray, and C. Kaiser, J. Phys. B **43**, 085202 (2010).
[28] M. K. Srivastava, R. K. Chauhan, and R. Srivastava, Phys. Rev. A **74**, 064701 (2006).
[29] U. Hitawala, G. Purohit, and K. K. Sud, J. Phys. B **41**, 035205 (2008).
[30] I. Bray, D. V. Fursa, and A. J. Stelbovics, J. Phys. B **41**, 215203 (2008).
[31] X. Jia and S. Sun, Phys. Rev. A **83**, 032715 (2011).
[32] Z. Li, Xu Shan, Jing Zhang, D. Meng, and Rui Wang, Phys. Lett. A **375**, 2563 (2011).
[33] A. J. Murray, Phys. Rev. A **72**, 062711 (2005).
[34] E. Clementi and C. Roetti, At. Data Nucl. Data Tables **14**, (1974).
[35] J. B. Furness and I. E. McCarthy, J. Phys. B **6**, 2280 (1973).
[36] M. E. Riley and D. G. Truhlar, J. Chem. Phys. **63**, 2182 (1975).
[37] I. E. McCarthy, Aust. J. Phys. **48**, 1 (1995).
[38] N. T. Padial and D. W. Norcross, Phys. Rev. A **29**, 1742 (1984).
[39] J. P. Perdew and A. Zunger, Phy. Rev. B **23**, 5048 (1981).
[40] J. Yuan and Z. Zhang, J. Phys. B **22**, 2751 (1989).
[41] S. J. Ward, and J. H. Macek, Phys. Rev. A **49**, 1049 (1994).
[42] G. H. Wannier, Phys. Rev. **90**, 817 (1953).
[43] M. R. H. Rudge, J. Phys. B **33**, 1223 (2000).
[44] S. Jones, D. H. Madison, and M. K. Srivastava, J. Phys. B **25**, 1899 (1992).
[45] F. A. Gianturco and S. Scialla, J. Phys. B **20**, 3171 (1987).
[46] R. K. Chauhan, M. K. Srivastava, and R. Srivastava, Phys. Rev. A **71**, 032708 (2005).